

Dear Editor,

Dear Authors,

This is a well written paper and I strongly support its publication in AMT without further delay after addressing a few minor issues as described in the following.

I also attach a version the manuscript where I inserted some of my comments in more detail.

Page 11058 (Review on different space-based isotopologue observations):

This is nice to have, but I would prefer to be a bit more careful and not put your deID data in the same category as the deID data obtained, for instance, by Herbin et al. (2009) or from SCIAMCHY and GOSAT (Frankenberg et al. 2013; Bösch et al., 2013). Your IASI retrieval, the MUSICA IASI retrieval, and the TES retrievals are very close to actual retrievals of deID (in the optimal estimation sense) and they use a fixed apriori (at least your retrieval and the MUSICA retrieval, for TES I also think so, but please check).

This is in contrast to the other approaches. There H<sub>2</sub>O and HDO are retrieved and then aposteriori the deID value is calculate from the retrieved H<sub>2</sub>O and HDO data. A so-obtained deID value depends on the differences between the H<sub>2</sub>O and HDO averaging kernels. This differences are changing (depend on the actual measurement situation, e.g., varying humidity). This is important for nadir looking satellites (for limb scanning instruments it is probably less important...). Furthermore some of those retrievals work with strongly varying aprioris and it is not sure what information of the deID product comes from the measurement and what is already there in the apriori assumption.

Maybe a good solution is to talk about your deID data (as well as the MUSICA IASI and TES data) as “retrieved deID” data and for the other data products avoid the term retrieved and just say “deID data are presented”, “give deID data”, or something similar.

Top of page 11061, bottom of page 11063

I would be happy to see here a very brief description/discussion of differences between your retrieval and the MUSICA IASI retrieval (Schneider and Hase, 2011; Wiegeler et al., 2014).

Fig. 6, A''hd kernel:

Did you consider that  $(\ln[\text{H}_2\text{O}] + \ln[\text{HDO}])/2$  or (H<sub>2</sub>O) variability is more than one order of magnitude larger than the  $\ln[\text{HDO}] - \ln[\text{H}_2\text{O}]$  (or deID) variability? Or did you just plot the A'' values? This needs to

be explained/discussed. In Schneider et al. (2012) and Wiegel et al. (2014) we multiply these  $A''_{hd}$  values by 12.5 in order to make the  $A''_{hd}$  kernel adequately comparable to the  $A''_{dd}$  kernel.

I ask this because your  $A''_{hd}$  values are extremely low if compared to the MUSICA products (Schneider et al., 2012; Wiegele et al., 2014).

Comparison between Fig. 6a and b:

This comparison is really nice and interesting and again clearly documents the great importance to have these  $A''$  kernels in order to understand the product. Thermal contrast is only one parameter that influences the kernels. Another is the vertical distribution of water vapour (or the temperature profile). In extreme cases, like very humid air at surface and much drier air above you very likely have also a maximum sensitivity shifted towards lower altitudes.

Page 11068, line 12:

You should give the formulae you actually use for calculating your errors (you do NOT work with your Equations 13-15!). I suggest citing here the Equation Numbers of Schneider et al. (2012) you are referring to.

LMDZiso – IASI comparison according to your Eqs. (16) and (17):

Here you do not consider the cross dependencies  $A''_{hd}$  and  $A''_{dh}$ .

Actually I think this is a good idea, because of “adding” the cross dependency to the smoothed you should consider them as a kind of error. They will then become visible in the comparison between LMDZiso and IASI.

Additional reference:

Wiegele et al. (2014):

A. Wiegele, M. Schneider, F. Hase, S. Barthlott, O. E. García, E. Sepúlveda, Y. González, T. Blumenstock, S. Dohe, M. Gisi, and R. Kohlhepp: “The MUSICA MetOp/IASI H<sub>2</sub>O and delD products: characterization and long-term comparison to NDACC/FTIR data”, accepted for AMTD.

Best regards,

Matthias Schneider

This discussion paper is/has been under review for the journal Atmospheric Measurement Techniques (AMT). Please refer to the corresponding final paper in AMT if available.

# Observation of tropospheric $\delta D$ by IASI over the Western Siberia: comparison with a GCM

M. Pommier<sup>1,2</sup>, J.-L. Lacour<sup>3</sup>, C. Risi<sup>4</sup>, F.-M. Bréon<sup>1</sup>, C. Clerbaux<sup>2,3</sup>, P.-F. Coheur<sup>3</sup>, K. Gribanov<sup>5</sup>, D. Hurtmans<sup>3</sup>, J. Jouzel<sup>1</sup>, and V. Zakharov<sup>5</sup>

<sup>1</sup>LSCE-IPSL, UMR8212, CEA-CNRS-UVSQ, CEA Saclay, 91191, Gif-sur-Yvette, France

<sup>2</sup>UPMC Univ. Paris 06; Université Versailles St-Quentin; UMR8190, CNRS/INSU, LATMOS-IPSL, Paris, France

<sup>3</sup>Spectroscopie de l'Atmosphère, Chimie Quantique et Photophysique, Université Libre de Bruxelles (ULB), Brussels, Belgium

<sup>4</sup>UPMC Univ. Paris 06; UMR8539, CNRS/INSU, LMD-IPSL, Paris, France

<sup>5</sup>Climate and Environmental Physics Laboratory, Ural Federal University, Russia

Received: 31 October 2013 – Accepted: 5 December 2013 – Published: 17 December 2013

Correspondence to: M. Pommier (matthieu.pommier@latmos.ipsl.fr)

Published by Copernicus Publications on behalf of the European Geosciences Union.

11055

## Abstract

This study presents the joint  $H_2^{16}O$  and HDO retrieval from Infrared Atmospheric Sounding Interferometer (IASI) spectra over the Western Siberia. IASI is an instrument on board the MetOp-A European satellite. The global coverage of the instrument and the good signal-to-noise ratio allow us to provide information on  $\delta D$  over this remote region. We show that IASI measurements may be used to estimate integrated  $\delta D$  between the surface and 3 km altitude or from 1 to 5 km depending on the thermal contrast, with observational errors lower than 4 % and 8 %, respectively. The retrieved data are compared to simulations from an isotopic GCM, LMDZ-iso over 2011. **The satellite measurements reproduce well the seasonal and day-to-day variations for  $\delta D$ ,** showing for the latter a good correlation with the model ( $r$  up to 0.8 with the smoothed data in summer). The IASI-based retrievals also show the seasonal variation of the specific humidity in both altitude ranges.

## 1 Introduction

Siberia covers 77 % of the Russian territory but it is almost unpopulated (3 inhab km<sup>-2</sup>). Siberia is important in the context of anthropogenic climate change which largely impacts this region (IPCC, 2007) mainly covered by tundra, forests, and lakes. The area has undergone a sharp increase of temperatures for the last decades, which in turn has induced changes the biogeochemical cycles and the hydrological cycle (e.g. Kane, 1997; Lapshina et al., 2001).

Water vapor is a key atmospheric compound and the dominant greenhouse gas in the Earth's atmosphere (Kiehl and Trenberth, 1997; Schmidt et al., 2010). It plays an important role in the radiative transfer (Hartmann, 2002; Soden and Held, 2006; Bony et al., 2006), the large-scale circulation (Sherwood et al., 2010), cloud formation (Luo and Rossow, 2004), precipitation (Bretherton et al., 2004), and stratospheric chemistry (Fueglistaler, 2009). The water cycle strongly controls various feedback mechanisms of

11056

the Earth system in response to perturbations of the energy balance of the troposphere, such as cloud and ice/snow-albedo feedbacks. The water cycle is also coupled to the surface energy budget by latent heat fluxes associated with evaporation and condensation. However, many aspects of the water cycle are still uncertain. The measurement

5 of the isotopic ratio of water, comparing the abundance of the heavier isotopologues (principally  $\text{H}_2^{18}\text{O}$ ,  $\text{H}_2^{17}\text{O}$  and HDO) to the main isotopologue  $\text{H}_2^{16}\text{O}$ , can provide an additional information about these processes and about the sources of water vapor.

Indeed, the chemical properties of all isotopologues are similar but their masses are different. There is a fractionation of the different isotopologues during evaporation/condensation processes due to the differences in vapour pressures and diffusivities in air.

The isotopic composition is given in per mil (‰) units using the conventional  $\delta$  notation relative to the V-SMOW standard (Vienna-Standard Mean Ocean Water). This is the reference standard for water isotope ratios (Craig, 1961). Our work focuses on  $\delta\text{D}$  as  $\delta^{18}\text{O}$  and  $\delta^{17}\text{O}$  are still challenging to retrieve from space.  $\delta\text{D}$  is expressed as below:

$$\delta\text{D} = 1000 \times \left( \frac{\text{HDO}/\text{H}_2\text{O}}{R_{\text{VSMOW}}} - 1 \right) \quad (1)$$

where  $R_{\text{VSMOW}} = 0.31152 \times 10^{-3}$ . Hence  $\delta\text{D}$  gives an indication on the abundance of HDO relative to that of  $\text{H}_2\text{O}$ . A  $\delta\text{D}$  of 0‰ indicates that the ratio is equal to that of sea water. A value of  $-500$ ‰ means that the ratio in the sample is only half that of the ratio in sea water, and a value of  $-1000$ ‰ means that the sample contains no HDO.

The study of the water isotopes has been carried out for many years in various scientific fields. The analysis in ice core improved our understanding of past climate (e.g. Jouzel et al., 2007). The spatial and temporal analysis of stable water isotopologues distribution in precipitation across the globe has a potential to improve our understanding of the hydrological cycle (e.g. Gat, 2000). In ecology, stable water isotopologues are used to evaluate soil evaporation, plant transpiration, drought effects on vegetation and

11057

water sources for different plants (e.g. Farquhar et al., 2007). These studies highlight the importance of a detailed understanding for the mechanism of the isotopic signal in atmospheric water vapor and thus on the improvement of its measurements.

In recent years the improvement in instrumental performances allowed to measure

5 the water vapor isotopic signal from the measurements acquired by spaceborne instruments with the Infrared Atmospheric Sounding Interferometer (IASI) among them. Herbin et al. (2009) showed first the possibility to detect  $\delta\text{D}$  with IASI and they analyzed the distribution during a typhoon event over South-East Asia, while Schneider and Hase (2011) performed a validation work over Tenerife and Lacour et al. (2012)

10 presented results for the 3–6 km distribution. Prior to IASI, the Interferometric Monitor for Greenhouse gases (IMG) (Zakharov et al., 2004; Herbin et al., 2007) and the Tropospheric Emission Spectrometer (TES) provided quasi-global distributions of  $\delta\text{D}$  representative of the mid-troposphere (e.g. Worden et al., 2006, 2007) whereas the Scanning Imaging Absorption spectrometer for Atmospheric Cartography (SCIAMACHY)

15 instrument provided total column distributions, with sensitivity down to the boundary layer (Frankenberg et al., 2009). Both TES and SCIAMACHY distributions required significant time averaging to reach the global scale, which puts a limit on what can be expected for monitoring short-term variability of water. The Thermal And Near infrared Sensor for carbon Observation – Fourier Transform Spectrometer (TANSO-FTS)

20 (e.g. Boesch et al., 2013; Frankenberg et al., 2013) can also be used to derive the  $\delta\text{D}$  total column distribution, and the Atmospheric Chemistry Experiment – Fourier Transform Spectrometer (ACE-FTS) gave information on the  $\delta\text{D}$  variability in the Tropical Tropopause Layer (Nassar et al., 2007).

This work documents for the first time  $\delta\text{D}$  retrievals from IASI radiances over land and at high latitudes. While the methodology to retrieve spectra measured above land was already developed in Lacour et al. (2012), the present dataset is interesting in that it includes cases with high thermal contrasts ( $\Delta T$ ) which greatly impact the sensitivity of the retrieval. Generally high latitudes retrievals are more challenging than low and mid- latitudes retrievals, mainly due to the cold temperature profiles of the atmosphere

and the lower concentration of water vapor that affect the information content present in the measurement. To cope with that difficulty, a specific a priori covariance matrix for high latitudes retrievals was built in order to better constrain the solutions of the inverse problem.

5 One of the rationales for the present study is to acquire a first IASI  $\delta D$  dataset for the high-latitude regions for comparison with model simulations, which have been suggested to have deficiencies at these high-latitudes (Risi et al., 2012a). Furthermore, models also underestimate the role of the continental recycling at mid-latitudes as over Siberia (e.g. Risi et al., 2013). Thanks to the joint effort from different communities  
10 within the Russian-French WSIBISO project (<http://wsibiso.ru>), the new dataset from IASI retrievals allows us to evaluate the performance of isotopic General Circulation Models (GCMs) over Siberia. Here we use the isotopic version of the LMDZ model, LMDZ-iso (Risi et al., 2010).

A global description of the IASI mission is given in Sect. 2. Section 3 presents the  
15 methodology used and provides a detailed characterization of the retrieved  $\delta D$ , under different thermal contrast conditions. The results are presented, compared with LMDZ-iso in Sect. 4. The conclusions are presented in Sect. 5.

## 2 Overview of IASI observations

IASI is a nadir-viewing Fourier Transform Spectrometer instrument. The first model  
20 (IASI-A), was launched in October 2006. The second instrument was launched in September 2012. The wide swath of the IASI instrument provides near global coverage twice daily with a local time of observation close to 9:30 a.m. and PM. IASI measures in the thermal infrared part of the spectrum, between 645 and 2760  $\text{cm}^{-1}$ . It records radiance from the Earth's surface and the atmosphere with an apodized spectral  
25 resolution of 0.5  $\text{cm}^{-1}$ , spectrally sampled at 0.25  $\text{cm}^{-1}$ . It has a low noise of 0.1–0.4 K for a reference blackbody at 280 K (Hilton et al., 2012), with the lower noise values in the range used for  $\delta D$  retrievals (e.g. Lacour et al., 2012). The IASI atmospheric view

11059

is composed of  $2 \times 2$  circular pixels each with a ground footprint of 12 km diameter at nadir and it has an across-track scan with a swath width of 2200 km. Owing to its large swath IASI provides a large number of observations per day even over small areas; this is illustrated for instance Fig. 1, which shows a sampling example around the city  
5 of Yekaterinburg for one day. This area is referred hereafter as YEK.

$\text{H}_2^{16}\text{O}$ ,  $\text{H}_2^{18}\text{O}$  and HDO are the three main isotopologues of water having large absorption bands in the thermal infrared region. Spectral signatures of these species are well detected by IASI. However, as explained by Herbin et al. (2009), a meaningful retrieval of the  $\text{H}_2^{18}\text{O}/\text{H}_2^{16}\text{O}$  is very challenging as its variation in the atmosphere is  
10 small. This is not the case for the HDO/ $\text{H}_2^{16}\text{O}$  ratio for which IASI was shown earlier to provide results of sufficient accuracy. In the following, we therefore focus on the retrievals of HDO and  $\text{H}_2^{16}\text{O}$  in order to study the  $\delta D$  variations. The selected spectral ranges are 1195–1223.5  $\text{cm}^{-1}$  and 1251.25–1253  $\text{cm}^{-1}$  (Fig. 2), avoiding the major interferences of  $\text{CH}_4$  and  $\text{N}_2\text{O}$ . In order to simplify the notations, the main isotopologue  
15  $\text{H}_2^{16}\text{O}$  will be named hereafter as  $\text{H}_2\text{O}$ .

As there are numerous IASI data (more than one million observations per day) and as the retrieval procedure for  $\delta D$  currently relies on a line-by-line approach that is computationally expensive, we have chosen to process only 1 pixel out of 4. Furthermore, only spectra with a cloud fraction (see IASI Level 2 Product Guide, 2008) below or  
20 equal to 10 % are considered and the few unrealistic positive retrieved  $\delta D$  values are filtered out. Overall this restricts the dataset to 9 % of the observations (15 234 out of 175 528) over the Siberia area for the year 2011. Despite these strict criteria and as shown in Fig. 1 for one day, the YEK area is still well covered by IASI.

## 3 Retrieval methodology summary

25 The methodology used to retrieve HDO/ $\text{H}_2\text{O}$  ratios from IASI radiances is overall similar to that presented in Lacour et al. (2012), which itself was stimulated by the earlier developments on the retrieval of  $\delta D$  presented by Schneider et al. (2006) and Worden

11060









(Fig. 6b)  $|\Delta T|$ . With their technique, the humidity and  $\delta D$  present the same vertical resolution and cross dependence between  $\delta D$  and  $\text{H}_2\text{O}$  is minimized. Even if the **DFS** is limited, this shows that IASI resolves the same air mass for both isotopologues. This transformation of the AKs sheds further light on the dependency of the retrieval to the local thermal contrast, with the  $\mathbf{A}''$  characterized by very different shapes. For low thermal contrast (Fig. 6a), the surface sensitivity for  $\delta D$  is vanishing and the information reduces to the integrated [1–5 km] column; the DFS is typically 0.7. When the thermal contrast is larger (Fig. 6b), the AK peaks at the surface and decrease rapidly, reaching very small values already at 4 km; the DFS is then slightly larger, around 0.8. Note; however, that the number of observations with large values of  $|\Delta T|$  is not so frequent so that on the yearly average, the most representative sensitivity is that depicted in Fig. 6a.

### 3.6.2 Error characterization

The error on the retrieval can be calculated as the difference between the retrieved state and the true state. Thus from the Eqs. (8) and (10) it is expressed as:

$$\hat{\mathbf{x}} - \mathbf{x} = (\mathbf{A} - \mathbf{I})(\mathbf{x} - \mathbf{x}_a) + \mathbf{G}\varepsilon + \mathbf{GK}(\mathbf{x} - \mathbf{x}_a) \quad (12)$$

The total error is so composed by three terms.  $(\mathbf{A} - \mathbf{I})(\mathbf{x} - \mathbf{x}_a)$  represents the smoothing error, which accounts for the vertical sensitivity of the measurements to the retrieved profile; the second term  $\mathbf{G}\varepsilon$  is the measurement error, associated to the spectral noise; and  $\mathbf{GK}(\mathbf{x} - \mathbf{x}_a)$  is the model parameters error representing the imperfect knowledge of the model parameters as temperature, water line-list of spectroscopic parameters or surface emissivity for example.

11067

Their covariance matrices are respectively given by:

$$\mathbf{S}_{\text{smoothing}} = (\mathbf{A} - \mathbf{I})\mathbf{S}_a(\mathbf{A} - \mathbf{I})^T \quad (13)$$

$$\mathbf{S}_{\text{measurement}} = \mathbf{G}\mathbf{S}_\varepsilon\mathbf{G}^T \quad (14)$$

$$\mathbf{S}_{\text{mod. param}} = \mathbf{GK}_b\mathbf{S}_b(\mathbf{GK}_b)^T \quad (15)$$

with  $\mathbf{S}_b$  representing uncertainty on the forward model parameters and  $\mathbf{K}_b$  is the sensitivity of the forward model to the forward parameters ( $= \frac{\partial \mathbf{F}}{\partial \mathbf{b}}$ ). In Eq. (13), the covariance matrix of a real ensemble of states generally approximated by the a priori covariance matrix  $\mathbf{S}_a$ . Equation (13) explicitly includes a vertical sensitivity through the  $\mathbf{A}$  matrix, and it is obvious that the smoothing error decreases when AKs are close to one and/or if the variability in  $\mathbf{S}_a$  is small.

Following the technique described by Schneider et al. (2012), we can determine directly the  $\delta D$  errors. The error budget for  $\text{H}_2\text{O}$  and  $\delta D$  is presented for both, a low (Fig. 7a) and a high (Fig. 7b) thermal contrast.

Reducing the vertical sensitivity of  $\text{H}_2\text{O}$  to the  $\delta D$  one gives a higher smoothing error for  $\text{H}_2\text{O}$  than considering the full sensitivity of  $\text{H}_2\text{O}$  ( $\mathbf{A}$ ). This smoothing error goes up to 55 % for  $\text{H}_2\text{O}$  and 5 % for  $\delta D$  close to the surface with a high  $|\Delta T|$ . In the mid-troposphere, with a low  $|\Delta T|$ , the smoothing error reaches 56 % for  $\text{H}_2\text{O}$  and 7 % for  $\delta D$ . Moreover the uncertainties on the temperature profile are the main sources on the total observational errors ([1–5 km]: < 15 % for  $\text{H}_2\text{O}$  and < 8 % for  $\delta D$  with a low  $|\Delta T|$ , [0–3 km]: < 6 % for  $\text{H}_2\text{O}$  and < 4 % for  $\delta D$  with a high  $|\Delta T|$ ).

## 4 Observations of the seasonal variability: comparison with a GCM

### 4.1 The isopotic General Circulation Model: LMDZ-iso

The resolution of the GCM LMDZ4 (Hourdin et al., 2006) used here is 2.5° in latitude, 3.75° in longitude and 19 vertical levels from the surface up to 3 hPa (~ 35 km). The

11068



conclusions from Risi et al. (2012b) and references therein. They highlighted the underestimation of the  $\delta D$  seasonal cycles by GCMs in mid and high latitudes.

LMDZ-iso also presents a bias on  $\delta D$  at mid and high latitudes with other atmospheric sounders as TES or TANSO-FTS (Risi et al., 2012a, 2013). The model underestimates the latitudinal gradient compared to these sounders (Risi et al., 2012a).  
5 There is an overestimation of  $\delta D$  by TANSO-FTS in summer, while this bias was less pronounced with TES. Nevertheless, the absolute  $\delta D$  values between both instruments are not directly comparable due to the lack of absolute validation. As suggested by Risi et al. (2013), the difference of sensitivity between all these instruments calls to perform  
10 more cross-validation exercises, not only on the mean  $\delta D$  but also on his variation.

### 4.3 Day-to-day variability

Section 4.2 shows the IASI performance to detect the seasonal cycle, both for  $\delta D$  and the specific humidity. On the time series shown in Figs. 8 and 9, a large fraction of the variability results from the seasonal cycle. To analyze whether the satellite data and the  
15 model agree on the synoptic variability, it is necessary to remove this cycle. We model the cycle as a cosine function that is fitted against the data. The synoptic variations are then derived from the original estimates by subtracting the seasonal cycle. The process and results are illustrated in Fig. 10 in lower altitudes and in Fig. 11 in the free troposphere. Figures 10a and 11a show the seasonal fit. Figures 10b and 11b show  
20 the  $\delta D$  deseasonalized cycle obtained for IASI, smoothed LMDZ-iso (convolved with the IASI AKs) and LMDZ-iso.

In the [0–3 km] altitude range, the variability obtained by the smoothed LMDZ values is underestimated by 2 compared to IASI one (Fig. 10b) but higher correlation are observed (Fig. 10c). This correlation is higher with the smoothed LMDZ distribution  
25 ( $r \sim 0.7$ ). The daily variability simulated by LMDZ in [1–5 km] is similar to that observed by IASI (Fig. 11b), in terms of both standard deviation and range. However, convolving with the AKs reduces the variability, so the smoothed LMDZ actually underestimates the daily variability compared to IASI one. Figure 11c shows the correlations between

11071

these daily averages values, with a good agreement ( $r \sim 0.6$  in both cases). For both altitudes range, the correlation is higher in summer (JJA) ( $r \sim 0.8$ ) (Table 1).

This shows that LMDZ-iso and IASI are also able to capture well the  $\delta D$  day-to-day variability and mostly in lower altitudes, confirming for the higher latitude what was  
5 shown earlier in tropical and sub-tropical regions (Lacour et al., 2012). The fact that two time series (LMDZ GCM and remotely sensed data) show a significant correlation provides some support to both of them even if the variability is underestimated with the smoothed values from the model. It does demonstrate that the short term variability does not result from random noise but is linked to true atmospheric processes.

### 4.4 Effect of thermal contrast on retrieved seasonal variations of the isotopic composition

As the IASI retrievals provide a good representation of the day-to-day variability, in agreement with the simulation from LMDZ-iso, they can be used to describe the isotopic composition in the air mass over Siberia. For this, we plot the  $\delta D$  values as a function  
15 of the specific humidity.

As described in the Sect. 3.6, the thermal contrast impacts on the vertical information provided by IASI. In our case, IASI is more sensitive close to the surface with a high thermal contrast, which occurs mainly in winter, and in the free troposphere with a low thermal contrast. Figure 12 shows the integrated  $\delta D$  and  $H_2O$  between 0 and 3 km,  
20 both for a  $|\Delta T| > 8$  K, and between 1 and 5 km for a  $|\Delta T| < 4$  K. In both cases, IASI detects well the seasonal change in the water isotopic composition with for example the depletion on  $\delta D$  in December-January-February between the surface and 3 km altitude.

## 5 Conclusions

This study is a contribution to the WSIBISO project. We have retrieved  $\delta D$  by IASI over land and more specifically over Siberia. The methodology is based on joint  $H_2^{16}O$  and HDO retrievals, elaborated by Lacour et al. (2012) and using the optimal estimation.  
5 15 234 retrieved spectra along the year 2011 over YEK.

A different a priori from Lacour et al. (2012) has been used. This a priori information has been built from a set of daily vertical profiles from the isotopic version of LMDZ GCM (LMDZ-iso), representative of the whole year at high latitudes.

IASI has shown his capability to measure the tropospheric  $\delta D$  at two different layers  
10 of the atmosphere according to the amplitude of the thermal contrast. IASI is more sensitive in the [0–3 km] altitude range with a high  $|\Delta T|$  (e.g. in January) and in the [1–5 km] altitude range with a low  $|\Delta T|$  (e.g. in July). These layers for which IASI is mostly sensitive complement of other  $\delta D$  measurements, performed by other satellite instruments and by ground-based measurements, which are sensitive to  $\delta D$  in different  
15 altitude range. We show that for the IASI retrievals, the total observational  $\delta D$  errors are lower than 4 % and 8 % close to the surface and in the free troposphere, respectively, with their respective thermal condition.

The data have been evaluated with the simulation from the LMDZ-iso GCM. IASI captures well the seasonal variation for the specific humidity and  $\delta D$  during 2011.  
20 IASI and the LMDZ-iso GCM show good agreement on  $\delta D$  following the posteriori processing from Schneider et al. (2012). We show that IASI is also able to observe the  $\delta D$  day-to-day variability and that the latter compares well with the model simulations ( $r \geq 0.6$ , up to 0.8 in summer) in both altitude ranges.

*Acknowledgements.* M. Pommier was supported by a fellowship grant from WSIBISO project (<http://wsibiso.ru>). This research was partly supported by a grant of the Russian government under the contract 11.G34.31.0064. P-F. Coheur is Senior Research Associate with FRS-FNRS. IASI was developed and built under the responsibility of Centre National des Etudes Spatiales (CNES) and flies onboard the MetOp satellite as part of the Eumetsat Polar system. The authors acknowledge the Ether French atmospheric database  
25 11073

(<http://www.pole-ether.fr/etherTypo/index.php?id=1450&L=1>) for providing the IASI L1C data.



The publication of this article is financed by CNRS-INSU.

## 5 References

- Boesch, H., Deutscher, N. M., Warneke, T., Byckling, K., Cogan, A. J., Griffith, D. W. T., Notholt, J., Parker, R. J., and Wang, Z.: HDO/ $H_2O$  ratio retrievals from GOSAT, *Atmos. Meas. Tech.*, 6, 599–612, doi:10.5194/amt-6-599-2013, 2013.
- Bony, S. and Emanuel, K. A.: A parameterization of the cloudiness associated with cumulus convection: evaluation using TOGA COARE data, *J. Atmos. Sci.*, 58, 3158–3183, 2001.
- 10 Bony, S., Colman, R., Kattsov, V. M., Allan, R. P., Bretherton, C. S., Dufresne, J.-L., Hall, A., Hallegatte, S., Holland, M. M., Ingram, W., Randall, D. A., Soden, B. J., Tselioudis, G., and Webb, M. J.: How well do we understand and evaluate climate change feedback processes?, *J. Climate*, 19, 3445–3482, 2006.
- 15 Bretherton, C. S., Peters, M. E., and Back, L. E.: Relationships between water vapor path and precipitation over the tropical oceans, *J. Climate*, 17, 1517–1528, 2004.
- Clerbaux, C., Boynard, A., Clarisse, L., George, M., Hadji-Lazaro, J., Herbin, H., Hurtmans, D., Pommier, M., Razavi, A., Turquety, S., Wespes, C., and Coheur, P-F: Monitoring of atmospheric composition using the thermal infrared IASI/MetOp sounder, *Atmos. Chem. Phys.*, 9, 6041–6054, doi:10.5194/acp-9-6041-2009, 2009.
- 20 Craig, H.: Isotopic variations in meteoric waters, *Science*, 133, 1702–1703, doi:10.1126/science.133.3465.1702, 1961.
- Emanuel, K. A.: A scheme for representing cumulus convection in large-scale models, *J. Atmos. Sci.*, 48, 2313–2329, 1991.
- 25 Emanuel, K. A. and Zivkovic-Rothman, M.: Development and evaluation of a convection scheme for use in climate models, *J. Atmos. Sci.*, 56, 1766–1782, 1999.

- Farquhar, G. D., Cernusak, L. A., and Barnes, B.: Heavy water fractionation during transpiration, *Plant Physiol.*, 143, 11–18, doi:10.1104/pp.106.093278, 2007.
- Frankenberg, C., Yoshimura, K., Warneke, T., Aben, I., Butz, A., Deutscher, N., Griffith, D., Hase, F., Notholt, J., Schneider, M., Schrijver, H., and Rockmann, T.: Dynamic Processes  
5 Governing Lower-Tropospheric HDO/H<sub>2</sub>O Ratios as Observed from Space and Ground, *Science*, 325, 1374–1377, doi:10.1126/science.1173791, 2009.
- Frankenberg, C., Wunch, D., Toon, G., Risi, C., Scheepmaker, R., Lee, J.-E., Wennberg, P., and Worden, J.: Water vapor isotopologue retrievals from high-resolution GOSAT shortwave infrared spectra, *Atmos. Meas. Tech.*, 6, 263–274, doi:10.5194/amt-6-263-2013, 2013.
- 10 Fueglistaler, S., Dessler, A. E., Dunkerton, T. J., Folkins, I., Fu, Q., and Mote, P. W.: Tropical tropopause layer, *Rev. Geophys.*, 47, RG1004, doi:10.1029/2008RG000267, 2009.
- Gat, J. R.: Atmospheric water balance – the isotopic perspective, *Hydrol. Process.*, 14, 1357–1369, doi:10.1002/1099-1085(20000615)14:8<1357:AID-HYP986>3.0.CO;2-7, 2000.
- Hartmann, D. L.: Climate Change: Tropical Surprises, *Science*, 295, 811–812, 2002.
- 15 Herbin, H., Hurtmans, D., Turquety, S., Wespes, C., Barret, B., Hadji-Lazaro, J., Clerbaux, C., and Coheur, P.-F.: Global distributions of water vapour isotopologues retrieved from IMG/ADEOS data, *Atmos. Chem. Phys.*, 7, 3957–3968, doi:10.5194/acp-7-3957-2007, 2007.
- Herbin, H., Hurtmans, D., Clerbaux, C., Clarisse, L., and Coheur, P.-F.: H<sub>2</sub><sup>16</sup>O and HDO measurements with IASI/MetOp, *Atmos. Chem. Phys.*, 9, 9433–9447, doi:10.5194/acp-9-9433-2009, 2009.
- 20 Hilton, F., Armante, R., August, T., Barnet, C., Bouchard, A., Camy-Peyret, C., Capelle, V., Clarisse, L., Clerbaux, C., Coheur, P.-F., Collard, A., Crevoisier, C., Dufour, G., Edwards, D., Faijan, F., Fourrié, N., Gambacorta, A., Goldberg, M., Guidard, V., Hurtmans, D., Illingworth, S., Jacquinet-Husson, N., Kerzenmacher, T., Klaes, D., Lavanant, L., Masiello, G., Matricardi, M., McNally, A., Newman, S., Pavelin, E., Payan, S., Péquignot, E., Peyridieu, S., Phulpin, T., Remedios, J., Schlüssel, P., Serio, C., Strow, L., Stubenrauch, C., Taylor, J., Tobin, D., Wolf, W., and Zhou, D.: Hyperspectral Earth Observation from IASI: five years of accomplishments, *B. Am. Meteorol. Soc.*, 93, 347–370, doi:10.1175/BAMS-D-11-00027.1, 2012.
- 30 Hourdin, F. and Armengaud, A.: The use of finite-volume methods for atmospheric advection of trace species, Part I: Test of various formulations in a General Circulation Model, *Mon. Weather Rev.*, 127, 822–837, 1999.

11075

- Hourdin, F., Musat, I., Bony, S., Braconnot, P., Codron, F., Dufresne, J.-L., Fairhead, L., Filiberti, M.-A., Friedlingstein, P., Grandpeix, J.-Y., Krinner, G., LeVan, P., Li, Z. X., and Lott, F.: The LMDZ4 general circulation model: climate performance and sensitivity to parametrized physics with emphasis on tropical convection, *Clim. Dynam.*, 27, 787–813, 2006.
- 5 IASI Level 2 Product Guide, EUM/OPS-EPS/MAN/04/0033, v2A, Eumetsat, 12 November 2008.
- IPCC: Contribution of Working Groups I, II and III to the Fourth Assessment Report of the Intergovernmental Panel on Climate Change, Core Writing Team, edited by: Pachauri, R. K., and Reisinger, A., Geneva, Switzerland, 104 pp., 2007.
- 10 Jouzel, J., Masson-Delmotte, V., Cattani, O., Dreyfus, G., Falourd, S., Hoffmann, G., Minster, B., Nouet, J., Barnola, J. M., Chappellaz, J., Fischer, H., Gallet, J. C., Johnsen, S., Leuenberger, M., Loulergue, L., Luethi, D., Oerter, H., Parrenin, F., Raisbeck, G., Raynaud, D., Schilt, A., Schwander, J., Selmo, E., Souchez, R., Spahni, R., Stauffer, B., Steffensen, J. P., Stenni, B., Stocker, T. F., Tison, J. L., Werner, M., and Wolff, E. W.: Orbital and millennial Antarctic climate variability over the past 800 000 years, *Science*, 317, 793–796, 2007.
- 15 Kane, D. L.: The impact of hydrologic perturbations on arctic ecosystems induced by climate change, in: *Global change and arctic terrestrial ecosystems*, edited by: Oechel, W. C., Callahan, T., Gilmanov, T., Holten, J. I., Maxwell, B., Molau, U., and Sveinbjörnsson, B., Springer-Verlag Inc., New York, 63–81, 1997.
- 20 Kiehl, J. T. and Trenberth, K. E.: Earth's annual global mean energy budget, *B. Am. Meteorol. Soc.*, 78, 197–208, doi:10.1175/1520-0477(1997)078<0197:EAGMEB>2.0.CO;2, 1997.
- Lacour, J.-L., Risi, C., Clarisse, L., Bony, S., Hurtmans, D., Clerbaux, C., and Coheur, P.-F.: Mid-tropospheric  $\delta D$  observations from IASI/MetOp at high spatial and temporal resolution, *Atmos. Chem. Phys.*, 12, 10817–10832, doi:10.5194/acp-12-10817-2012, 2012.
- 25 Lapshina, E. D., Velichko, A. A., Borisova, O. K., Kremenetsky, K. V., and Pologova, N. N.: Holocene dynamics of peat accumulation, in: *Carbon Storage and Atmospheric Exchange by west Siberian Peatlands*, edited by: Bleuten, W. and Lapshina, E. D., FGU Scientific Reports 2001-1, Utrecht (NL), ISBN 90-806594-1-X p47-72, 2001.
- 30 Luo, Z. and Rossow, W. B.: Characterizing tropical cirrus life cycle, evolution, and interaction with upper-tropospheric water vapor using Lagrangian trajectory analysis of satellite observations, *J. Climate*, 17, 4541–4563, 2004.

11076

- Nassar, R., Bernath, P. F., Boone, C. D., Gettelman, A., McLeod, S. D., and Rinsland, C. P.: Variability in HDO/H<sub>2</sub>O abundance ratios in the tropical tropopause layer, *J. Geophys. Res.*, 112, 1–11, doi:10.1029/2007JD008417, 2007.
- Risi, C., Bony, S., Vimeux, F., and Jouzel, J.: Water stable isotopes in the LMDZ4 General Circulation Model: model evaluation for present day and past climates and applications to climatic interpretation of tropical isotopic records, *J. Geophys. Res.*, 115, D12118, doi:10.1029/2009JD013255, 2010.
- Risi, C., Noone, D., Worden, J., Frankenberg, C., Stiller, G., Kiefer, M., Funke, B., Walker, K., Bernath, P., Schneider, M., Wunch, D., Sherlock, V., Deutscher, N., Griffith, D., Wennberg, P. O., Strong, K., Smale, D., Mahieu, E., Barthlott, S., Hase, F., García, O., Notholt, J., Warneke, T., Toon, G., Sayres, D., Bony, S., Lee, J., Brown, D., Uemura, R., and Sturm, C.: Process-evaluation of tropospheric humidity simulated by general circulation models using water vapor isotopologues: 1. Comparison between models and observations, *J. Geophys. Res.*, 117, D05303, doi:10.1029/2011JD016621, 2012a.
- Risi, C., Noone, D., Worden, J., Frankenberg, C., Stiller, G., Kiefer, M., Funke, B., Walker, K., Bernath, P., Schneider, M., Bony, S., Lee, J., Brown, D., and Sturm, C.: Process-evaluation of tropospheric humidity simulated by general circulation models using water vapor isotopic observations: 2. Using isotopic diagnostics to understand the mid and upper tropospheric moist bias in the tropics and subtropics, *J. Geophys. Res.*, 117, D05304, doi:10.1029/2011JD016623, 2012b.
- Risi, C., Noone, D., Frankenberg, C., and Worden, J.: Role of continental recycling in intraseasonal variations of continental moisture as deduced from model simulations and water vapor isotopic measurements, *Water Resour. Res.*, 49, 4136–4156, doi:10.1002/wrcr.20312, 2013.
- Rodgers, C. D.: *Inverse methods for atmospheric sounding: theory and practise*, World Scientific, 2000.
- Rothman, L. S., Barbe, A., Chris Benner, D., Brown, L. R., Camy-Peyret, C., Carleer, M. R., Chance, K., Clerbaux, C., Dana, V., Devi, V. M., Fayt, A., Flaud, J. M., Gamache, R. R., Goldman, A., Jacquemart, D., Jucks, K. W., Lafferty, W. J., Mandin, J. Y., Massie, S. T., Nemtchinov, V., Newnham, D. A., Perrin, A., Rinsland, C. P., Schroeder, J., Smith, K. M., Smith, M. A. H., Tang, K., Toth, R. A., Vander Auwera, J., Varanasi, P., and Yoshino, K.: The HITRAN molecular spectroscopic database: edition of 2000 including updates through 2001, *J. Quant. Spectrosc. Ra.*, 82, 5–44, 2003.

11077

- Schmidt, G. A., Ruedy, R. A., Miller, R. L., and Lacis, A. A.: Attribution of the present-day total greenhouse effect, *J. Geophys. Res.*, 115, D20106, doi:10.1029/2010JD014287, 2010.
- Schneider, M. and Hase, F.: Optimal estimation of tropospheric H<sub>2</sub>O and δD with IASI/METOP, *Atmos. Chem. Phys.*, 11, 11207–11220, doi:10.5194/acp-11-11207-2011, 2011.
- Schneider, M., Hase, F., and Blumenstock, T.: Ground-based remote sensing of HDO/H<sub>2</sub>O ratio profiles: introduction and validation of an innovative retrieval approach, *Atmos. Chem. Phys.*, 6, 4705–4722, doi:10.5194/acp-6-4705-2006, 2006.
- Schneider, M., Yoshimura, K., Hase, F., and Blumenstock, T.: The ground-based FTIR network's potential for investigating the atmospheric water cycle, *Atmos. Chem. Phys.*, 10, 3427–3442, doi:10.5194/acp-10-3427-2010, 2010.
- Schneider, M., Barthlott, S., Hase, F., González, Y., Yoshimura, K., García, O. E., Sepúlveda, E., Gomez-Pelaez, A., Gisi, M., Kohlhepp, R., Dohe, S., Blumenstock, T., Wiegeler, A., Christner, E., Strong, K., Weaver, D., Palm, M., Deutscher, N. M., Warneke, T., Notholt, J., Lejeune, B., Demoulin, P., Jones, N., Griffith, D. W. T., Smale, D., and Robinson, J.: Ground-based remote sensing of tropospheric water vapour isotopologues within the project MUSICA, *Atmos. Meas. Tech.*, 5, 3007–3027, doi:10.5194/amt-5-3007-2012, 2012.
- Sherwood, S. C., Ingram, W., Tsushima, Y., Satoh, M., Roberts, M., Vidale, P. L., and O’Gorman, P. A.: Relative humidity changes in a warmer climate, *J. Geophys. Res.*, 115, D09104, doi:10.1029/2009JD012585, 2010.
- Soden, B. J. and I. M. Held: An assessment of climate feedbacks in coupled ocean-atmosphere models, *J. Climate*, 19, 3354–3360, doi:10.1175/JCLI3799.1, 2006.
- Van Leer, B.: Towards the ultimate conservative difference scheme: IV a new approach to numerical convection, *J. Comput. Phys.*, 23, 276–299, 1977.
- Worden, J., Bowman, K., Noone, D., Beer, R., Clough, S., Eldering, A., Fisher, B., Goldman, A., Gunson, M., Herman, R., Kulawik, S. S., Lampel, M., Luo, M., Osterman, G., Rinsland, C., Rodgers, C., Sander, S., Shephard, M., and Worden, H.: Tropospheric emission spectrometer observations of the tropospheric HDO/H<sub>2</sub>O ratio: estimation approach and characterization, *J. Geophys. Res.-Atmos.*, 111, D16309, doi:10.1029/2005jd006606, 2006.
- Worden, J., Noone, D., and Bowman, K.: Importance of rain evaporation and continental convection in the tropical water cycle, *Nature*, 445, 528–532, doi:10.1038/nature05508, 2007.
- Worden, J., Kulawik, S., Frankenberg, C., Payne, V., Bowman, K., Cady-Peirara, K., Wecht, K., Lee, J.-E., and Noone, D.: Profiles of CH<sub>4</sub>, HDO, H<sub>2</sub>O, and N<sub>2</sub>O with improved lower tro-

11078

ospheric vertical resolution from Aura TES radiances, Atmos. Meas. Tech., 5, 397–411, doi:10.5194/amt-5-397-2012, 2012.

- Zakharov, V. I., Imasu, R., Gribanov, K. G., Hoffmann, G., and Jouzel, J.: Latitudinal distribution of deuterium ratio in the atmospheric water vapor retrieved from IMG/ADEOS data, Geophys. Res. Lett., 31, L12104, doi:10.1029/2004GL019433, 2004.

11079

**Table 1.** Correlation coefficients between the deseasonalized smoothed LMDZ and IASI  $\delta D$ , and between the deseasonalized LMDZ and IASI  $\delta D$  for 4 seasons and both altitude ranges (0–3 km and 1–5 km).

	DJF	MAM	JJA	SON
<i>r</i> 0–3 km (smoothed)	0.42	0.71	0.8	0.65
<i>r</i> 0–3 km	0.23	0.72	0.84	0.58
<i>r</i> 1–5 km (smoothed)	0.19	0.66	0.8	0.46
<i>r</i> 1–5 km	0.06	0.67	0.78	0.53

11080

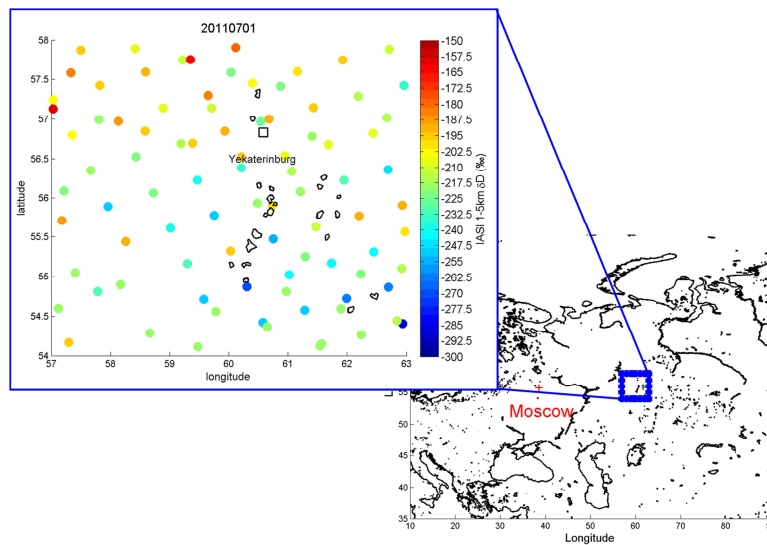


**Fig. 1.** IASI cloud-free observation of 1–5 km  $\delta D$  (in ‰) over the Yekaterinburg area (YEK) on 1 July 2011; only 1 pixel out of four is processed and shown. Each circle represents the observation at the location of the center of each pixel. The city is marked with the square.

11081

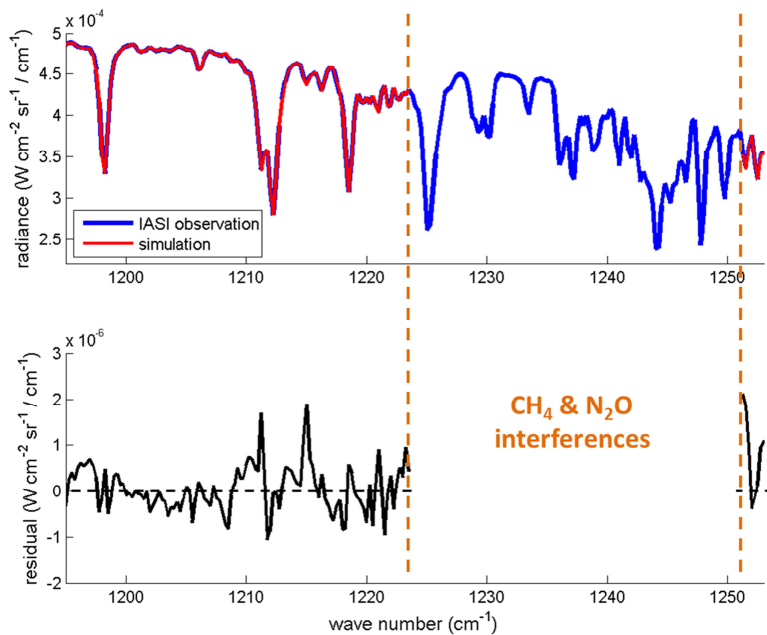


**Fig. 2.** Upper panel: IASI observed spectra (blue curve), the calculated spectra (red curve) in radiance units for August 2011. Bottom panel: The corresponding residual is plotted in black, with a RMS of  $1.05 \times 10^{-6} \text{ W cm}^{-2} \text{ sr}^{-1} / \text{cm}^{-1}$ . Note the factor 100 between the residual and the radiance. The gap on the residual highlights the part where the retrieval is not performed, avoiding major  $\text{CH}_4$  and  $\text{N}_2\text{O}$  interferences.

11082



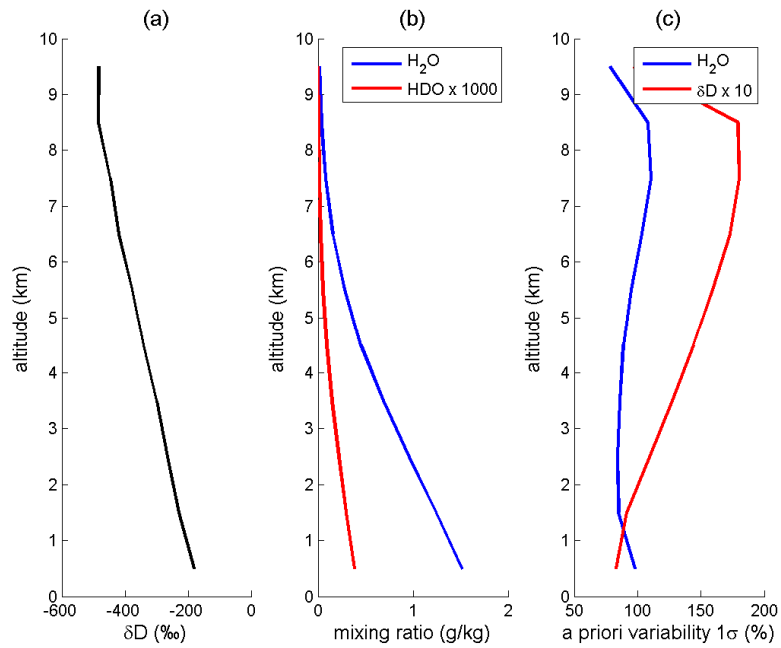


**Fig. 3.** A priori profiles used in the retrieval for  $\delta D$  in ‰ (a), for  $H_2O$  and HDO (in  $g\ kg^{-1}$ ), plotted in blue and red curves, respectively (b). The a priori variability  $1\sigma$  for  $H_2O$  and  $\delta D$  are expressed in % (c).

11083

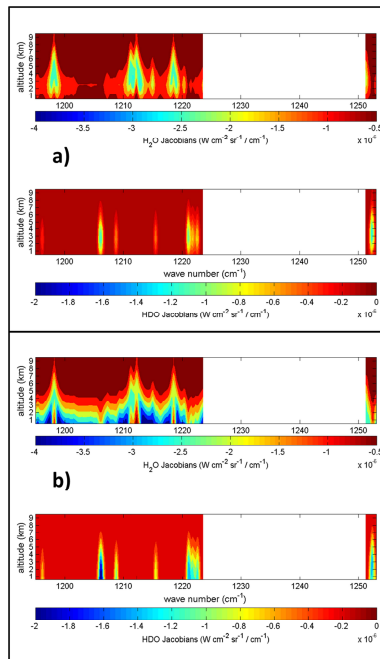


**Fig. 4.** Monthly Jacobian means of  $H_2O$  (upper panel) and HDO (bottom panel) as a function of altitude and wavenumber for July 2011 with a low ( $< 4\ K$ ) (a) and a large ( $> 8\ K$ ) absolute value of thermal contrast. The smallest derivatives values indicate the maximum sensitivities (dark blue). As Fig. 2, the gap highlights the part where the retrieval is not performed, avoiding major  $CH_4$  and  $N_2O$  interferences.

11084

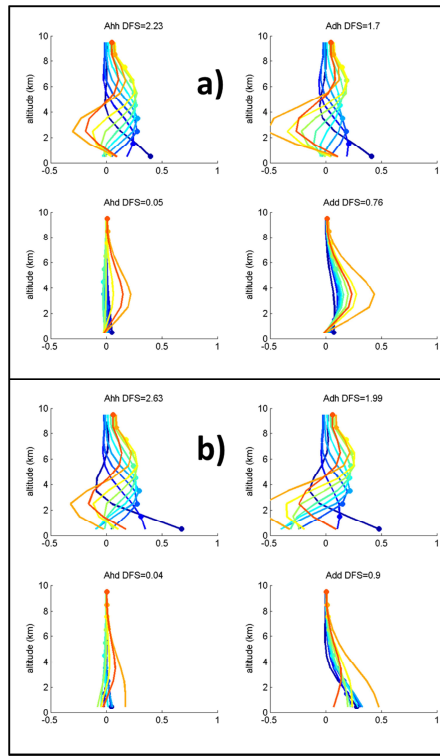


**Fig. 5.** Mean AKs (**A**) with a  $|\Delta T| < 4$  K (**a**) and with a  $|\Delta T| > 8$  K (**b**) on 2011. See text for the definition of  $A_{hh}$ ,  $A_{dd}$ ,  $A_{hd}$  and  $A_{dh}$  and for the explanation of both panels. The colored curves and dots aim to help the reader to follow the variability of each AK with altitude.

11085

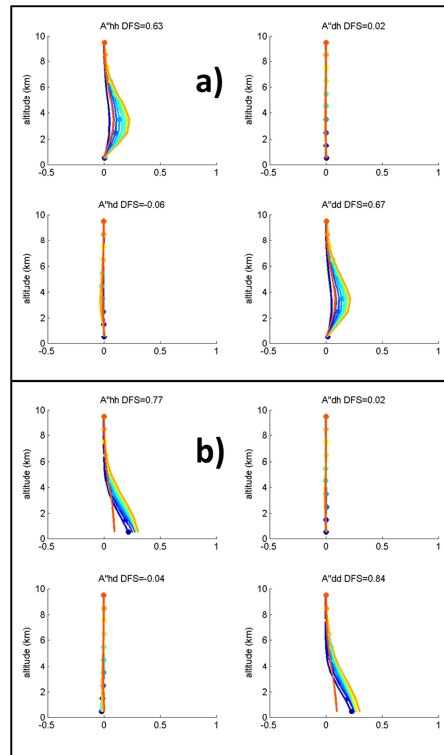


**Fig. 6.** As Fig. 5 for  $A''$ , representing the {humidity, proxy- $\delta D$ } state.

11086

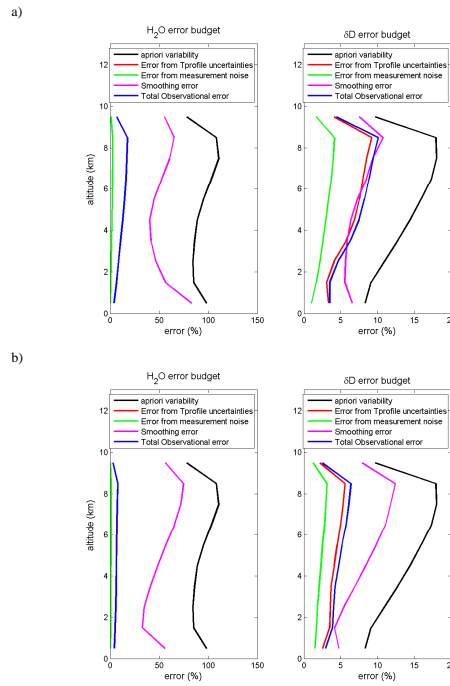


**Fig. 7.** Mean error profiles (quadratic sum of covariance) on 2011 with  $|\Delta T| < 4$  K **(a)** and  $|\Delta T| > 8$  K **(b)** for air temperature, measurement noise, smoothing, and the total observational ( $\sqrt{\text{temperature}^2 + \text{measurement noise}^2}$ ), for  $\text{H}_2\text{O}$  (left) and  $\delta D$  (right) for the {humidity, proxy- $\delta D$ } state.

11087

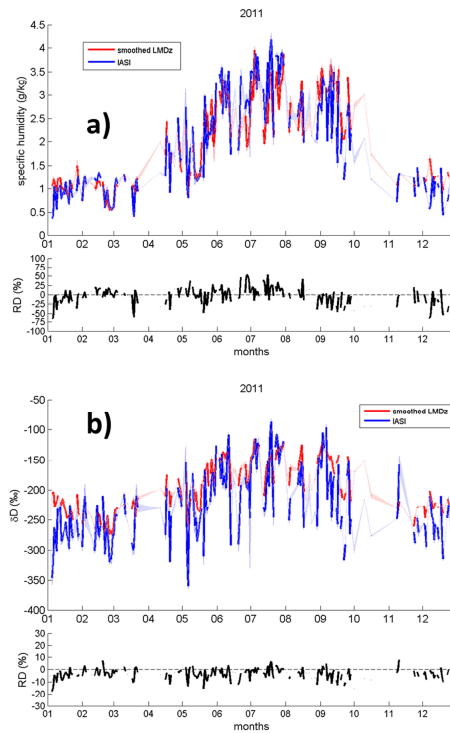


**Fig. 8.** Daily [0–3 km] specific humidity **(a)** and  $\delta D$  **(b)** means by IASI (blue curve) and smoothed LMDZ-iso (red curve) in 2011 with a  $|\Delta T| > 8$  K. The shade contour represents the standard deviation. The relative difference is calculated as:  $((\text{IASI}-\text{LMDZ-iso})/\text{LMDZ-iso}) \times 100\%$ . For the  $\text{RD}_{\delta D}$  calculation,  $\delta D$  is normalized by  $\delta D + 1000$ .

11088

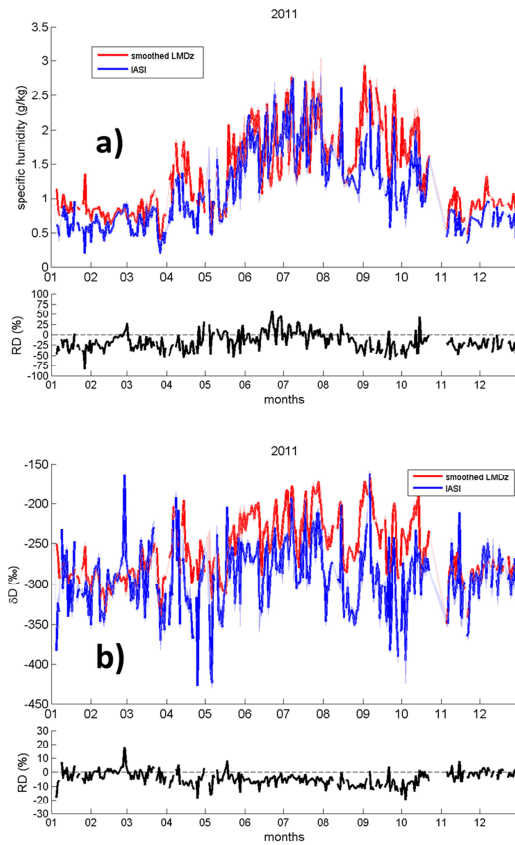


Fig. 9. As Fig. 8 for [1–5 km] with a  $|\Delta T| < 4$  K.

11089

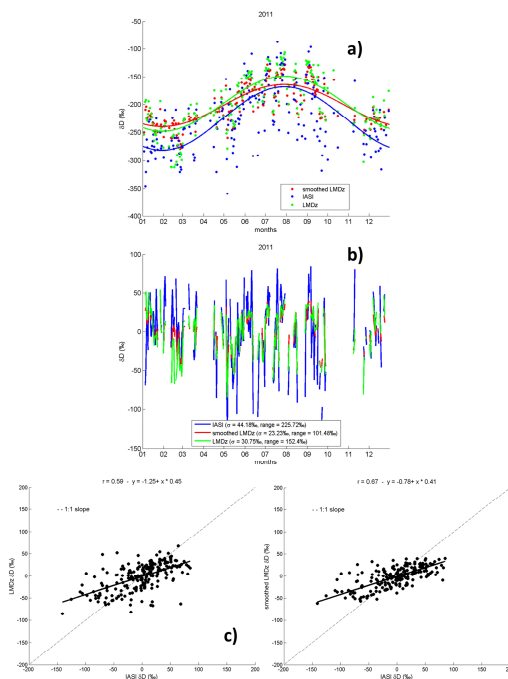
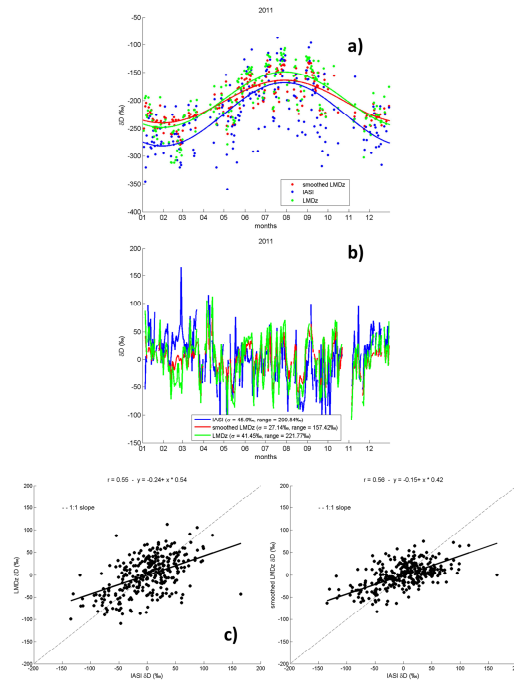


Fig. 10. (a) Daily [0–3 km]  $\delta D$  means for IASI (blue), smoothed LMDZ-iso (red) and LMDZ-iso (green) with their seasonal trend (curve) in 2011 with a  $|\Delta T| > 8$  K. This seasonal fit is defined as:  $\delta D = \overline{\delta D} + \text{std}(\delta D) \times \cos\left(\frac{2\pi}{360} \times (\text{day} - 210)\right)$ . (b)  $\delta D$  deseasonalized time series obtained by subtracting daily means time series by the seasonal fit. (c) Scatterplot between the deseasonalized daily mean data (left: LMDZ-iso vs. IASI, right: smoothed LMDZ-iso vs. IASI). The dashed line corresponds to the theoretical 1 : 1 slope and the black line corresponds to the linear regression.

11090



**Fig. 11.** As Fig. 10 for [1–5 km] with a  $|\Delta T| < 4$  K.

11091

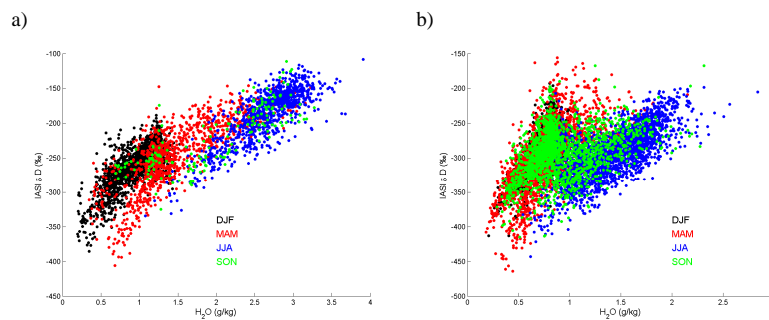


**Fig. 12.** IASI  $\delta D$  as function of  $H_2O$  ( $g\,kg^{-1}$ ) for the four seasons between 0 and 3 km when  $|\Delta T| > 8$  K (a) and between 1 and 5 km when  $|\Delta T| < 4$  K (b).

11092